Scientific Research Publishing

Open Journal of Civil Engineering, 2025, 15(1), 91-112
https://www.scirp.org/journal/ojce
ISSN Online: 2164-3172
ISSN Print: 2164-3164

Quantifying Failure Surface Roughness and Fractal Characteristics in Open-Pit Mining: The Case of Mashamba West Mine

Dina Kon[1], Jisen Shu[2], Liu Han[2], Sage Ngoie[3]

[1]Department of Mining Engineering, China University of Mining and Technology, Xuzhou, China
[2]State Key Laboratory of Resources and Mine Safety, China University of Mining & Technology, Xuzhou, China
[3]Department of Mining Geology, University of Kolwezi, Lualaba, DR Congo
Email: dinakon25@gmail.com

How to cite this paper: Kon, D., Shu, J.S., Han, L. and Ngoie, S. (2025) Quantifying Failure Surface Roughness and Fractal Characteristics in Open-Pit Mining: The Case of Mashamba West Mine. *Open Journal of Civil Engineering*, **15**, 91-112.
https://doi.org/10.4236/ojce.2025.151006

Received: January 12, 2025
Accepted: March 14, 2025
Published: March 17, 2025

Abstract

This study investigates the surface roughness and fractal properties of failure surfaces at the Mashamba West mine to enhance the understanding of the complex topographical features that influence slope stability in open-pit mining. Traditional methods for quantifying surface roughness, such as the mean absolute deviation (MAD) and standard deviation (SD), often fail to capture the multiscale and correlated behaviors typical of natural surfaces. In this research, advanced techniques, including fractal dimension calculations, semi-variogram and box-counting methods, and power spectral density (PSD) analysis, were employed to provide a more accurate characterization of the failure surface. The results revealed significant micro-roughness, with a mean absolute deviation of 0.83 and a standard deviation of 1.04, indicating a high level of surface irregularity. Geometric irregularities, such as pronounced asperities and depressions, were identified through the analysis of topographical extremes, with a mean peak height of 2.4828 and a mean valley depth of −4.7747. Fractal analysis, performed using both semi-variogram and box-counting methods, confirmed the self-affine nature of the failure surface with fractal dimensions of 1.5634 and 2.0735, respectively, indicating scale-invariant roughness patterns. The power spectral density analysis revealed a dominant frequency corresponding to periodic geological structures. These findings provide valuable insights into the surface characteristics of failure zones and offer a robust framework for future slope stability analysis. This study contributes to the field by demonstrating the utility of fractal analysis in characterizing complex failure surfaces and lays the groundwork for future research on the relationship between surface roughness and mechanical behavior in open-pit mining contexts.

Keywords

Surface Roughness, Fractal Dimension, Slope Stability, Open-Pit Mining, Geotechnical Modeling

1. Introduction

Surface topography significantly affects the mechanical properties and mode of failure of failure surfaces in open-pit slopes and their shear strength [1]-[4]. These surface properties must be appropriately quantified and understood to estimate the forces in geological materials and to design efficient mitigation strategies to enable safe mining operations [5] [6]. Although the mean absolute deviation (MAD) and standard deviation (SD) are reasonable starting points for surface variability, they are insufficient to fully describe the multiscale and correlated characteristics of natural surfaces [7]-[11]. Open-cast mine slopes are formed by geological processes such as weathering, faulting, and jointing, thus forming a complex surface that may exhibit similar patterns at different scales [12]-[15]. Such multiscale characteristics are directly important for the mechanical behavior of rock masses, thus requiring sophisticated techniques for their characterization [16]-[20]. Conventional methods assume statistical independence and only deal with localized properties. This makes them inadequate for analyzing surfaces governed by long-range dependencies and complex scaling laws [21]-[26]. However, these complexities have been captured by fractal geometry, a concept introduced by Mandelbrot [27]. Fractal dimensions, with their potential to quantify surface patterns and address the limitations of other roughness measures in the context of slope stability predictions, offer a promising future for geotechnical engineering [28]-[34]. The fractal dimension is a scale-independent parameter that measures the surface complexity to analyze the self-similar and multiscale characteristics of failure surfaces [34]. Other methods, including power spectral density (PSD) analysis [35], variogram analysis [36] [37], and box-counting [38]-[40], can be used to gain a better understanding of surface topography. These tools help to evaluate the frequency-domain characteristics, spatial dependencies, and scaling properties of the surface. These sophisticated methods are valuable in geotechnical engineering, particularly open-cast mining [41]. Variogram and box-counting methods are most useful in quantifying spatial scaling and self-affine characteristics, which are very important in mechanical interaction at the local and global scales [21] [36] [38]. These advanced techniques have improved the accuracy of geotechnical models and have dealt with the restrictions of traditional methods [30] [42] [43]. High fractal dimensions indicate highly irregular, anisotropic surfaces that tend to fail, whereas low dimensions are associated with smooth and stable surfaces [44] [45]. Thus, it is possible to identify potential failure zones by analyzing the short- and long-range dependence [38] [39].

Although MAD and SD are valuable, they are based on the assumption of sta-

tistical independence and do not consider the geological interactions and dependencies present in the system. The failure to consider these factors highlights the need for more sophisticated tools, including PSD analysis, variogram analysis, and box-counting, which can provide a more holistic understanding of both frequency and spatial domain properties. However, even with these additional tools, it can still be challenging to fully characterize the complexity of natural failure surfaces. Therefore, this research, which aims to determine the fractal characteristics of failure surfaces and their roughness, is of utmost importance for slope stability assessment in open-pit mining. The significance of this research lies in its potential to revolutionize the fields of geotechnical engineering and open-cast mining. This study was divided into four parts. The first part of this study characterized the roughness of the failure surfaces and their fractal dimensions. The second section will examine how lithology influences surface roughness and, in turn, slope stability. The third part will apply fractal and spectral analyses to validate its application in assessing slope stability. The fourth part will incorporate fractal dimensions into conventional slope stability analysis methods.

2. Location and Geological Condition of the Study Area

The study area is located within the Kolwezi Nappe in the Central African Copperbelt, approximately 7 km southwest of Kolwezi City in Katanga Province, Democratic Republic of Congo (DRC). This site encompasses the Mashamba West mining section, which is a crucial part of the Kolwezi thrust-and-fold belt. Regional geology and geomorphology strongly influence mining operations, making this location ideal for studying the slope stability and geological heterogeneity. The Mashamba West mine lies in the southeastern part of the Manika Plateau, a subsection of the Katanga Plateau, at altitudes ranging from 1375 to 1525 m. The area features gently undulating terrain with an overall gradient declining from southeast to northwest. The tropical savanna climate, characterized by distinct wet and dry seasons, governs geomorphological processes. The average annual rainfall is 1188 mm, primarily from November to March, which impacts surface erosion and slope stability. Geologically, the mine is part of the western section of the Central African Copperbelt, a globally recognized metallogenic zone. The Kolwezi complex thrust-and-fold belt comprises various lithostratigraphic units, primarily from the Roan Supergroup, which hosts stratiform copper-cobalt mineralization. Quantitative geological data highlight the complex structural framework of the region, where fault density is approximately 0.3 faults per kilometer, indicating a highly fractured rock mass. The joint spacing varies between 0.5 and 1.2 m, and plays a critical role in influencing the slope shear strength and deformation mechanisms. The structural orientation is dominated by axial folds and thrust faults with consistent orientations of 30˚ - 40˚NE, reflecting significant tectonic compression. The bedrock lithology included weathered dolomites, siltstones, shales, and silicified formations. These lithologies exhibit differential weathering patterns and mechanical behaviors that influence the self-affine characteristics of the slope

surfaces. The hydrogeological conditions in Mashamba West are significant because the site hosts multiple aquifers embedded within fractured dolomitic and sandstone units. These aquifers contribute significantly to the groundwater pressure, which is a critical factor in slope instability. Piezometric measurements indicate varying hydrostatic conditions influenced by local structural settings, with the permeability of primary aquifers ranging from 10^{-6} to 10^{-4} m/s. Groundwater levels in the mine vary between 1406.68 m and 1407.44 m, which directly affects slope stability. Mining activities in Mashamba West have induced considerable geomorphological changes. The pit, spanning an area of 0.89 km^2 and reaching a depth of 134 m, exhibits steep slopes. These slopes are dominated by loose soft materials, leading to frequent collapses and instabilities, as shown in Figure 1. Tailings and waste rock dumps in proximity exacerbate stress redistribution along slope boundaries, further complicating stability concerns. This detailed understanding of the geological and hydrogeological conditions of Mashamba West underscores the necessity for integrated geotechnical and fractal analyses to effectively address the challenges associated with slope stability. Enhanced visual aids such as geological maps and hydrogeological schematics are recommended to comprehensively illustrate complex structural and lithological settings.

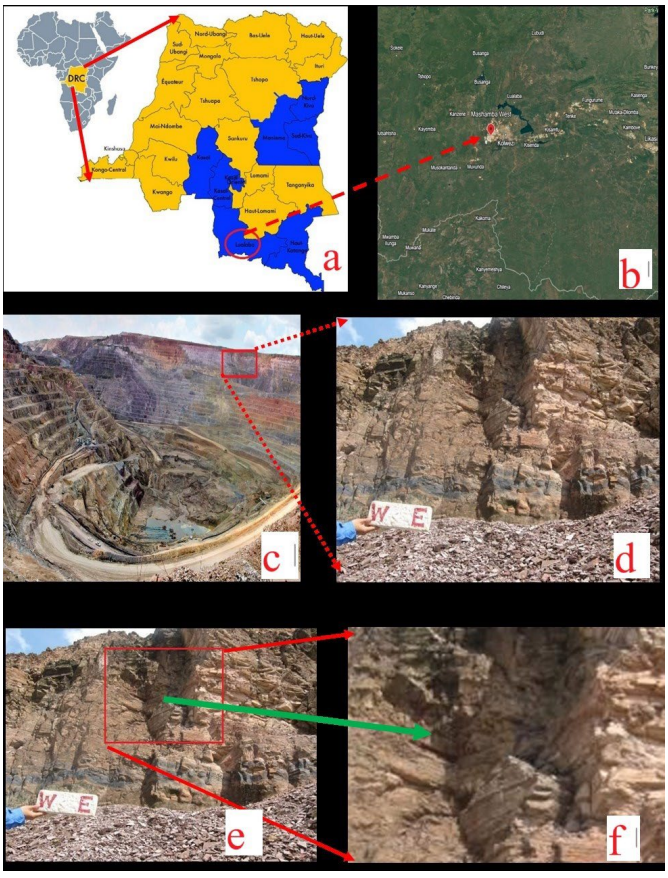

Figure 1. Location of the study area: (a) DRC map; (b) Kolwezi province map obtained from Google Earth; (c) Mashamba West mine; (d) study zone in the Mashamba West mine; (e) Region of interest; (f) failure surface.

3. Surface Roughness Description

Surface roughness is crucial for understanding the mechanical behavior of failure surfaces in open-pit mining, as it directly affects factors such as shear strength, frictional resistance, and slope stability. There are two primary reasons for measuring surface roughness in this context: first, to ensure accurate material characterization for better predictive modeling and second, to assess how these roughness characteristics influence failure mechanisms and slope stability in mining operations [2]. In open-pit mining, surface roughness is related to both the structural integrity of rock masses and the effectiveness of stabilization strategies.

Rough surfaces in mining are characterized by two key geometric aspects:

- Random Aspect: Roughness can vary significantly in space in a random manner, with no simple spatial function capable of fully describing the surface's geometric form. This randomness complicates the traditional methods of surface characterization, which require more sophisticated techniques such as fractal geometry.
- Structural Aspect: The roughness variations are not independent across the surface; rather, they exhibit spatial correlations that depend on the distance. Periodic patterns may emerge in geological contexts, particularly in rock surfaces affected by weathering, jointing, and faulting. These patterns are often associated with underlying geological structures, which influence the failure mechanisms observed in open-pit mining.

In this study, the surface roughness was quantified through an analysis of the surface height variation (SHV) traces, which can provide numerous roughness parameters. Classical roughness parameters are typically based on a set of points $R(d_i)$, which $i = 1, \cdots, M$, defined within a sample-length interval L. These measurement points, d_j, were selected equidistantly, and the roughness at each point was represented by the variable R_j. To identify positions along the length scale, it is sufficient to determine the sampling distance $d_S = d_j - d_{j-1} = L/M$ for $j > 1$. This methodology is useful for characterizing failure surface roughness in open-pit mining and for identifying scaling behaviors that can influence slope stability. The standard roughness parameters used frequently in practice are as follows:

3.1. Mean Absolute Deviation (MAD) and Mean Standard Deviation (MSD)

The mean absolute deviation (MAD) measures the average absolute deviation of the surface heights from the mean height. It is defined as:

$$\mathrm{MAD} = \frac{1}{K}\sum_{i=1}^{K}\left|S_i - S\right| \tag{3-1}$$

where S_i represents the surface heights at equidistant points i, S is the mean surface height, and K is the total number of points. MAD offers a direct measure of roughness and is particularly effective when surface elements are statistically

independent. The mean standard deviation (MSD), given by:

$$\mathrm{MSD} = \sqrt{\frac{1}{K}\sum_{i=1}^{K}\left(S_i - S\right)^2} \tag{3-2}$$

Equation (3-2) offers insights into the variability of surface heights and is particularly advantageous for assessing the normal distributions in surface-height data. MSD is particularly advantageous for assessing the variability of surface heights when they follow a normal distribution (**Figure 2**). These metrics are essential for probabilistic slope stability analyses because they quantify the surface variability that affects shear resistance.

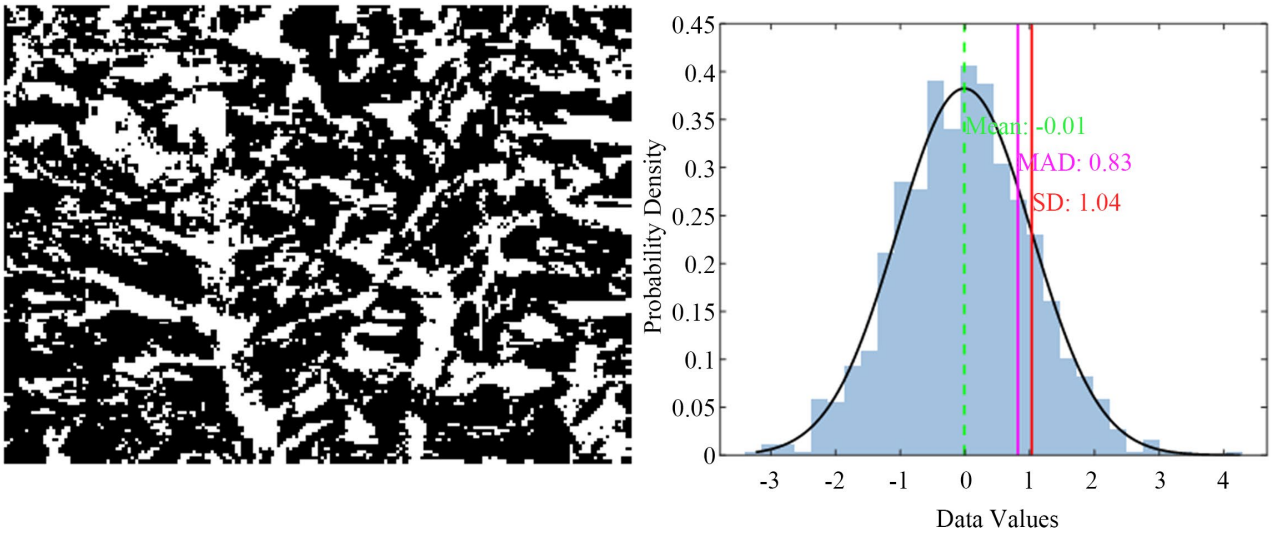

Figure 2. Failure surface image of the western part of Mashamba West: (a) canny edge detection; (b) data distribution with MAD and MSD for Failure Surface.

3.2. Peak and Valley Analysis

To evaluate the localized geometry of the failure surfaces, parameters such as mean peak height (M_P) and mean valley depth (M_V) were calculated as follows:

$$M_P = \frac{1}{K_p}\sum_{i=1}^{K_p} P_i, \quad P_i = \max\left(0, S_i - S\right) \tag{3-3}$$

$$M_V = \frac{1}{K_v}\sum_{i=1}^{K_v} V_i, \quad V_i = \max\left(0, S - S_i\right) \tag{3-4}$$

where K_p indicates the total number of peaks in the surface profile, K_v is the total number of valleys in the surface profile, and P_i is the height of the ith peak above the mean height S. where S_i is the height of the surface profile at the ith measurement point, S is the mean height of the surface profile, and V_i is the depth of the ith valley below the mean height as in **Figure 3**.

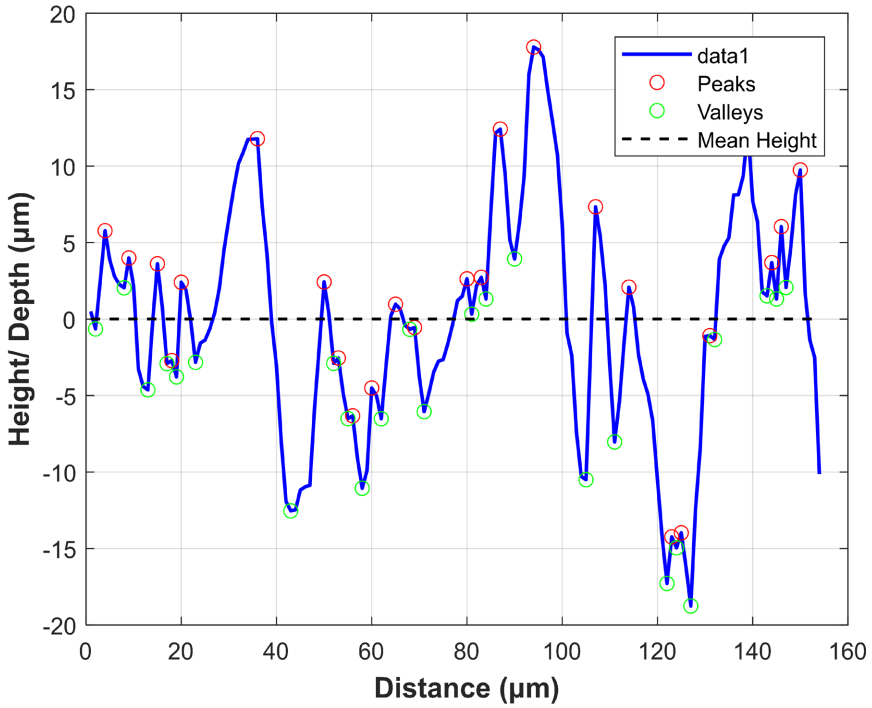

Figure 3. Surface profile with identified peaks and valleys.

3.3. Slope and Curvature Analysis

Parameters such as the standard deviation of the slope (PS) and curvature (PC) provide insights into the geometric irregularities of failure surfaces. These are defined as:

$$\mathrm{PS} = \sqrt{\frac{1}{K}\sum_{i=1}^{K}\left(\frac{\mathrm{d}S_i}{\mathrm{d}x}\right)^2} \tag{3-5}$$

$$\mathrm{PC} = \sqrt{\frac{1}{K}\sum_{i=1}^{K}\left(\frac{\mathrm{d}^2S_i}{\mathrm{d}x^2}\right)^2} \tag{3-6}$$

PS is the standard deviation of the slope of the surface profile, which measures the average variation in the slope of the failure surface, reflecting its roughness; K is the total number of equidistant points i sampled along the failure surface profile; $\frac{\mathrm{d}S_i}{\mathrm{d}x}$ is the slope of the surface profile at the ith point, representing the first derivative of the surface height (S_i) with respect to the spatial coordinate x; PC is the standard deviation of the curvature of the surface profile, which quantifies the average variation in the curvature of the failure surface, which is indicative of its waviness; $\frac{\mathrm{d}^2S_i}{\mathrm{d}x^2}$ is the curvature of the surface profile at the ith point, representing the first derivative of the surface height (R_j) with respect to the spatial coordinate x. These parameters are crucial for characterizing the roughness of the failure surface (**Figure 4**).

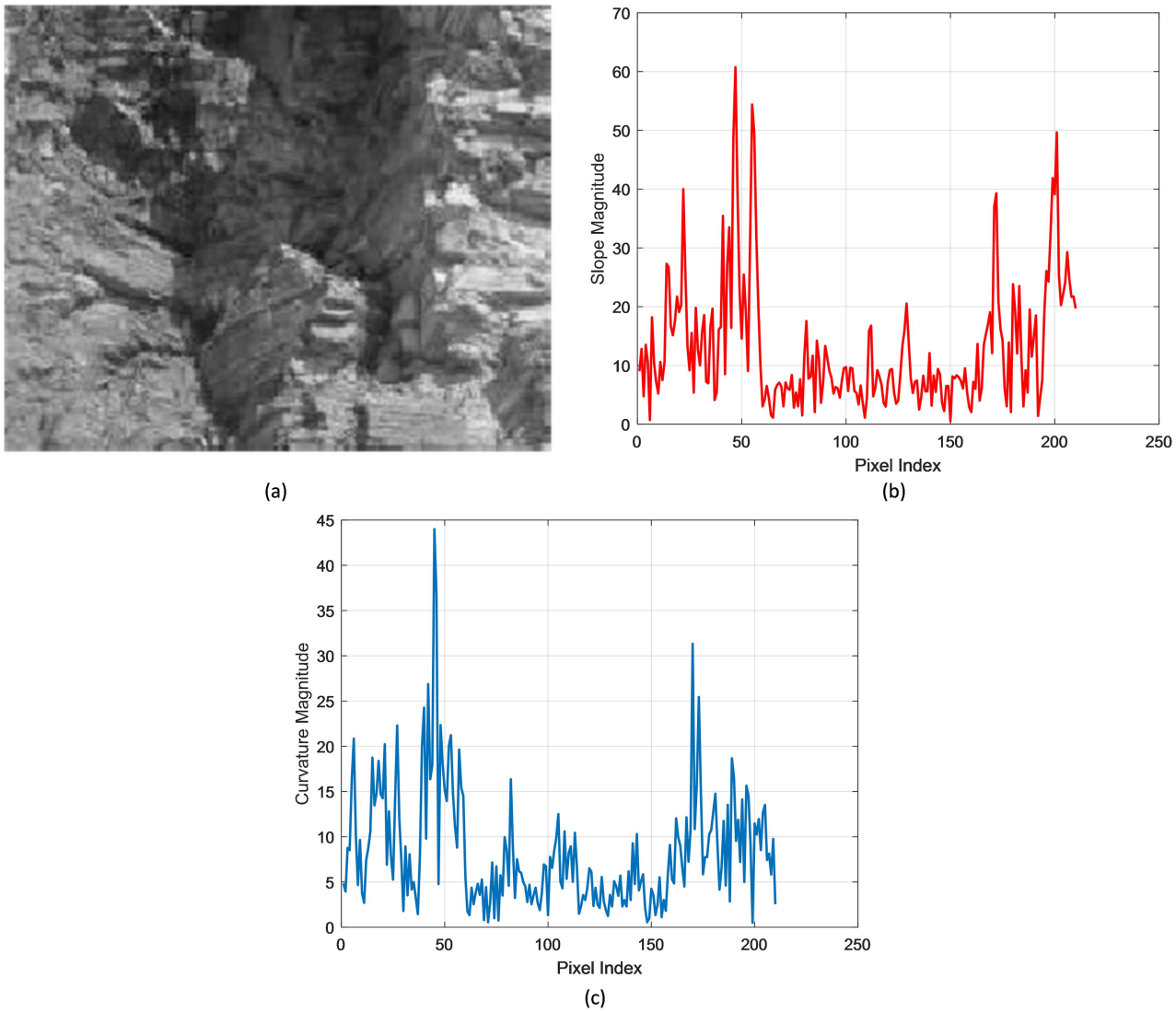

Figure 4. Slope and curvature analysis: (a) grayscale image of failure surface; (b) slope magnitude of the profile; (c) curvature magnitude of the profile.

3.4. Spectral Analysis

Spectral analysis of the failure surfaces is an essential tool for characterizing periodicities and roughness properties. Failure surfaces often exhibit spatial variability that can be decomposed into frequency components, thereby revealing the underlying patterns and effects of geological structures as shown in **Figure 5**. For a failure surface, the surface height variation can be expressed as a Fourier series:

$$R_m = \frac{a_0}{2} + \sum_{\lambda=1}^{n} \left[a_\lambda \cos\left(2\pi\lambda m\right) + b_\lambda \sin\left(2\pi\lambda m\right) \right] \tag{3-7}$$

where m is the spatial distance along the failure surface, a_λ, and b_λ are the Fourier coefficients representing the contributions of each frequency component. The frequencies of $\lambda = 1, 2, 3, \cdots$ correspond to periodic features of the surface, such as joints, fractures, or bedding planes. The power spectral density (PSD) de-

rived from the Fourier transform quantifies the contribution of each frequency to the total surface variability. It is computed as:

$$P_{\omega} = \frac{\left|R_F(\omega)\right|^2}{L^2} \tag{3-8}$$

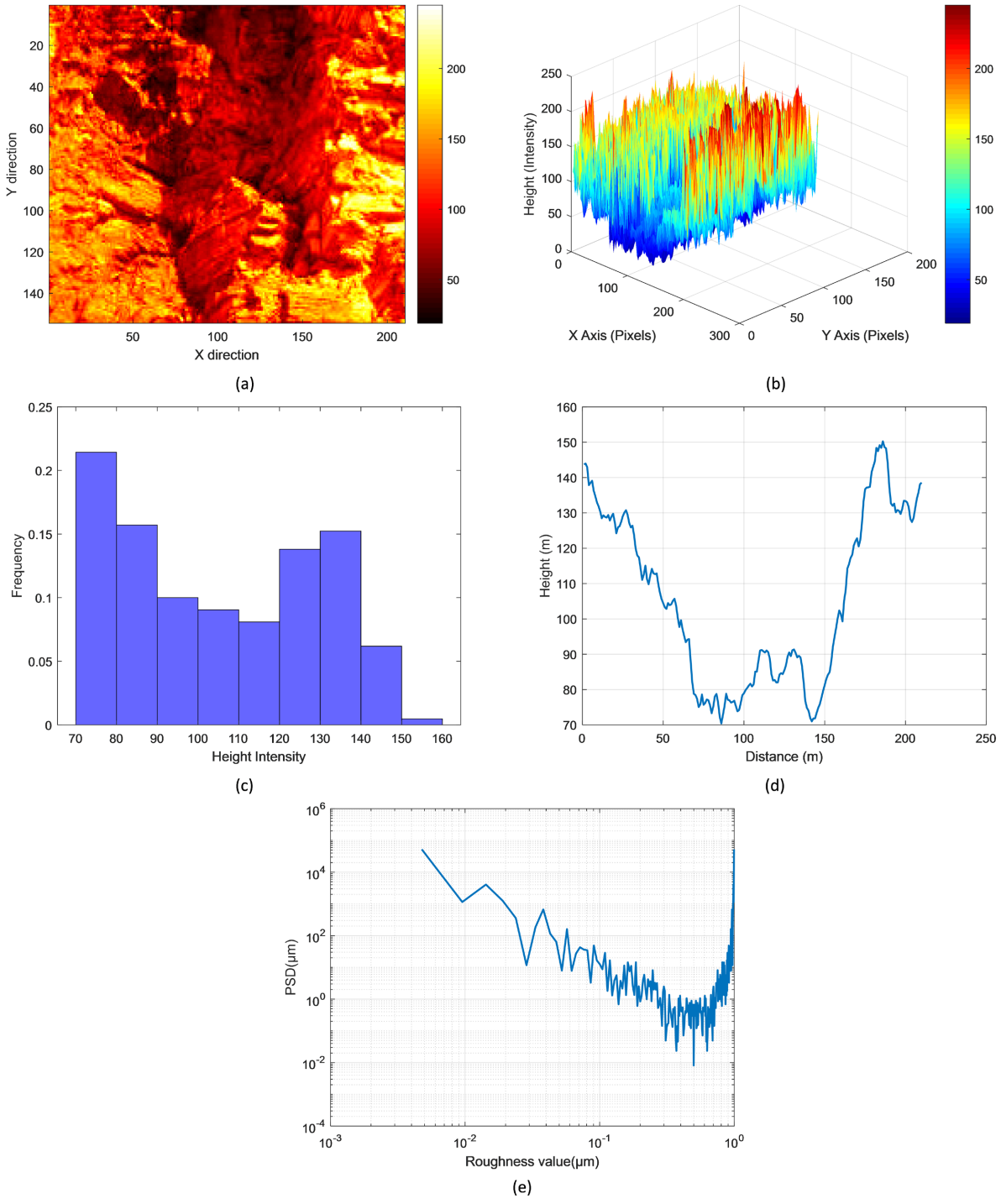

Figure 5. Correlation matrix of roughness parameters for failure surface analysis: (a) heatmap of failure surface; (b) surface plot of failure surface in 3D; (c) histogram of surface profile; (d) surface profile; (e) power spectral density.

where $R_F(\omega)$ is the Fourier transform of $R(d)$, ω is the spatial frequency, and L is the length of the analyzed surface profile. The PSD function enables the identification of dominant frequencies associated with structural features that can influence the slope stability. The spectral analysis process for failure surfaces typically involves several preprocessing steps to ensure accurate results. First, the raw surface height data must be detrended to remove non stationary components, such as large-scale inclinations or curvatures unrelated to roughness. The detrended data are then multiplied by a window function, such as a Hamming or parabolic window, to reduce the spectral leakage. Spectral leakage occurs owing to the finite length of the surface profile, which distorts the frequency content in PSD. The dependence of $\log(P_\omega)$ on $\log(\omega)$ provides valuable insights into surface roughness characteristics. For fractal-like failure surfaces, this relationship is often linear, which indicates self-affine properties. The slope S of the linear segment is related to the fractal dimension D of the surface:

$$S = -(2D-1) \tag{3-9}$$

To simulate the spectral estimators applied to the failure surface, a periodic structure with added random noise $N(0,1)$ can be used to model the spatial variability of the surface. The simulated failure surface height variation $R(d)$ along the slope profile can be represented as follows:

$$R_m = 3\sin(2\pi\times 10\cdot m) + 4\sin(2\pi\times 4\cdot m) + N(0,0.1) \tag{3-10}$$

R_m is the surface height variation at spatial distance m, $3\sin(2\pi\times 10\cdot m)$, and $4\sin(2\pi\times 4\cdot m)$, the periodic components corresponding to structural characteristics such as joint spacing or bedding planes; $N(0,0.1)$ is a Gaussian random noise component with a mean of 0 and a standard deviation of 0.1, simulating irregularities and stochastic variations typical of natural failure surfaces. This simulated profile captures both periodic geological features and random surface roughness, thereby providing a basis for evaluating the effectiveness of spectral estimators in characterizing the geometric and fractal properties of the failure surface. The choice of $N(0,1)$ or $N(0,0.1)$ in a simulation depends on the desired magnitude of noise relative to the signal and the physical characteristics of the modeled failure surface.

3.5. Statistical Analysis

Statistical analysis of failure surfaces on slopes provides critical insights into spatial correlations and variability. The primary tools used in this analysis include the autocorrelation function (ACF) and variogram, both of which are used to assess the relationships between surface heights at various spatial separations or lag distances (**Figure 6**). The autocorrelation function (ACF) quantifies the degree of similarity between surface height measurements separated by a lag distance t, which is calculated as:

$$\mathrm{ACF}(t) = \frac{\sum_{i=1}^{N-t}\left(S(d_i)-S\right)\left(S(d_{i+t})-S\right)}{\sum_{i=1}^{N}\left(S(d_i)-S\right)} \tag{3-11}$$

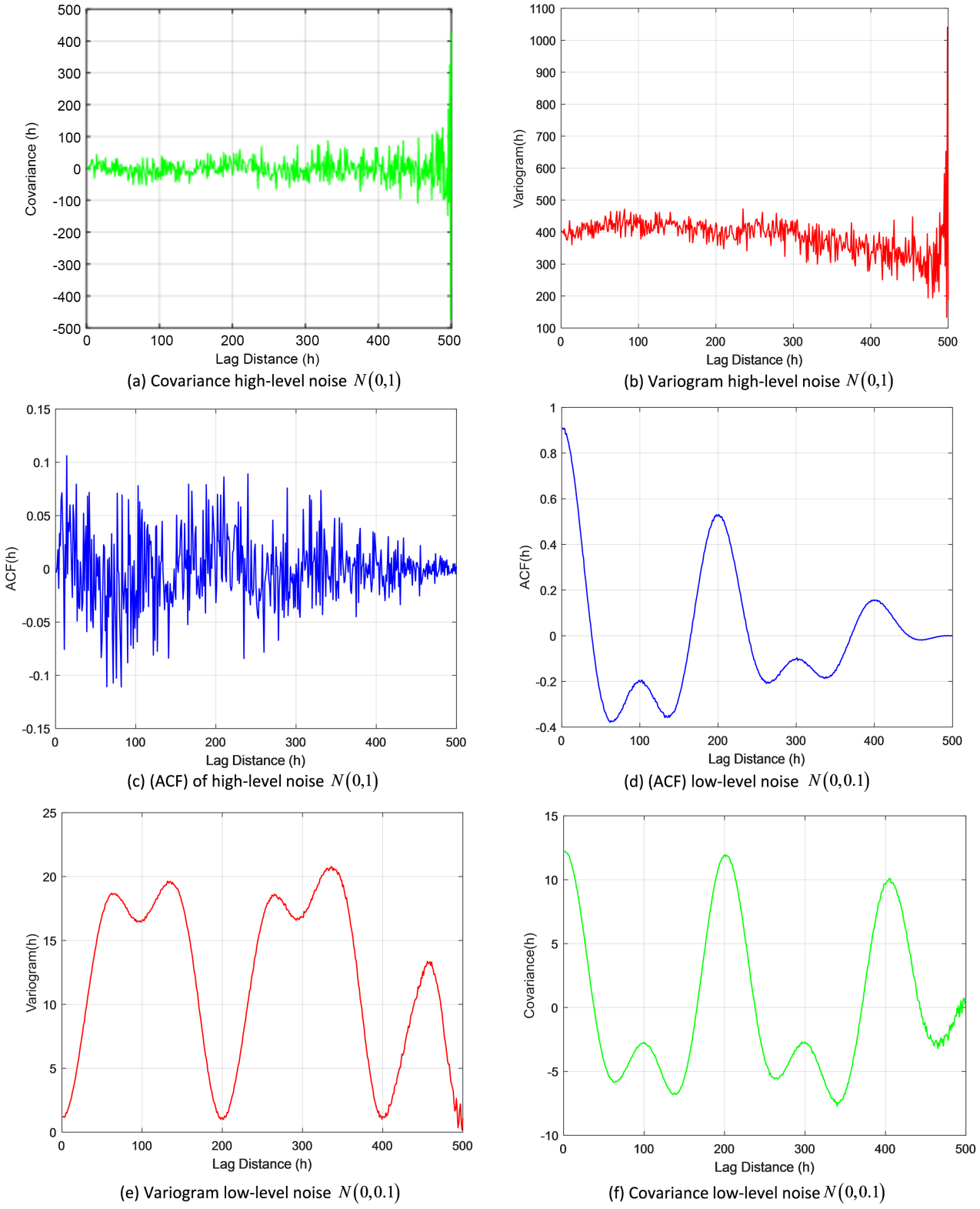

(a) Covariance high-level noise $N(0,1)$

(b) Variogram high-level noise $N(0,1)$

(c) (ACF) of high-level noise $N(0,1)$

(d) (ACF) low-level noise $N(0,0.1)$

(e) Variogram low-level noise $N(0,0.1)$

(f) Covariance low-level noise $N(0,0.1)$

Figure 6. Statistical analysis of failure surfaces: (a) covariance high-level noise $N(0,1)$; (b) variogram high-level noise $N(0,1)$; (c) (ACF) of high-level noise $N(0,1)$; (d) (ACF) low-level noise $N(0,0.1)$; (e) variogram low-level noise $N(0,0.1)$; (f) covariance high-level noise $N(0,0.1)$.

where $S(d_i)$ and $S(d_{i+t})$ are the surface heights at positions d_i and d_{i+h}, S is the mean height, and N is the number of data points. For failure surfaces, ACF reveals how roughness features are spatially correlated, with longer correlation lengths indicating more uniform roughness. The variogram measures the variance in the surface height differences over a range of lag distances. It is defined as:

$$\gamma_t = \frac{1}{2N_t}\sum_{i=1}^{N_t}\left[S(d_i) - S(d_{i+t})\right]^2 \tag{3-12}$$

where γ_t is the variogram value for lag t, and N_t is the number of point pairs separated by t. For failure surfaces, the variogram is useful for identifying spatial scaling properties and structural anisotropy. Statistical measures, such as variance and covariance, further describe the variability and spatial dependencies of the surface roughness. The covariance function is defined as follows:

$$U_t = \frac{1}{N_t}\sum_{i=1}^{N_t}\left[\left(S(d_i) - S\right)\left(S(d_{i+t}) - S\right)\right] \tag{3-13}$$

where U_t represents the covariance between the surface heights at a lag distance t. The relationship between the covariance function and variogram is given by:

$$\gamma_t = U_0 - U_t \tag{3-14}$$

where U_0 is the variance in the surface height data. For failure surfaces, these statistical tools are applied to characterize roughness, detect anisotropic features, and evaluate the degree of spatial correlation, all of which can influence mechanical behavior. For instance, high variability or short correlation lengths in roughness can lead to localized weaknesses, whereas a uniform roughness over longer distances can provide greater shear resistance. The analysis of ACF and the variogram was further extended by fitting fractal or power-law models to quantify the scaling behavior. This is particularly useful for surfaces exhibiting self-affinity, where the relationship between the variogram and the lag distance is as follows:

$$\gamma_t \alpha t^{2H} \tag{3-15}$$

H is the Hurst value, which is related to the fractal dimension D_f of the failure surface. The spatial characteristics of the failure surfaces were effectively captured by applying these statistical methods.

4. Estimation of the Fractal Dimension

4.1. Box-Counting Method

The box-counting method is widely used due to its simplicity in mathematical calculation and empirical estimation (Falconer, 1990). To determine the box-counting dimension D_B of a bounded subset Γ in $\mathbb{R}^n$, a mesh of squares or boxes with side length ε is overlaid on the set, and the number $N(\varepsilon)$ of these elements intersecting Γ is counted (Falconer, 1990). By varying the scale ε, different values of $N(\varepsilon)$ are obtained. If the surface exhibits fractal behavior, the relationship between $N(\varepsilon)$ and ε is given by:

$$N(\varepsilon) \sim \varepsilon^{-D_B} \tag{4-1}$$

where D_B denotes the fractal dimension of the failure surface. A logarithmic transformation of this relationship yields a linear plot, where the slope corresponds to the $-D_B$. The box-counting dimension is expressed as follows:

$$D_B = -\lim_{\varepsilon \to 0} \frac{\ln N(\varepsilon)}{\ln \varepsilon} \tag{4-2}$$

The value $N(\varepsilon)$, representing the number of mesh elements intersecting the set at a given scale ε, serves as an indicator of the spatial irregularity or complexity of the failure surface [46].

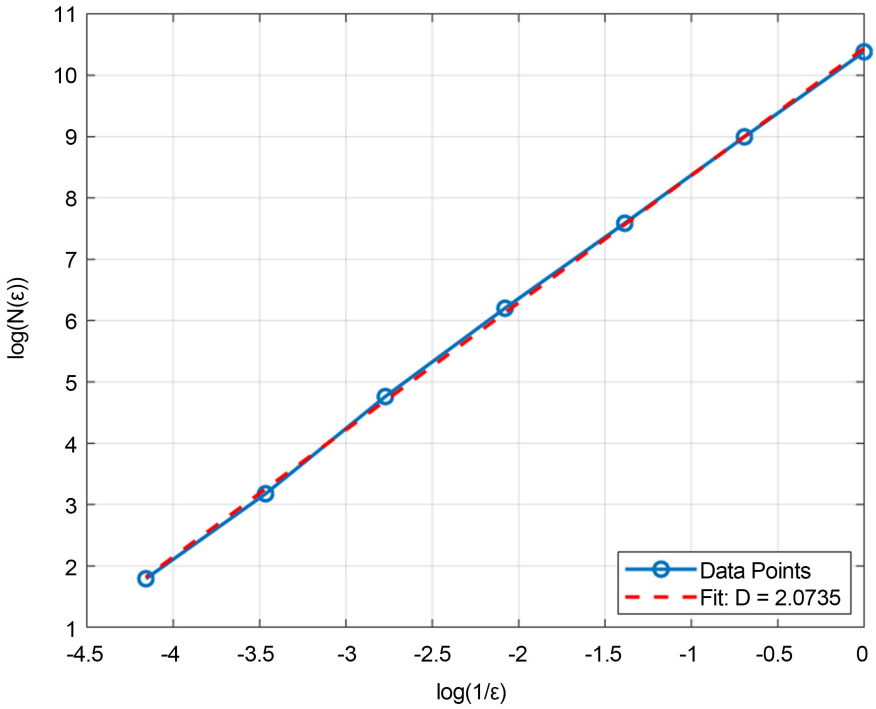

Figure 7. Fractal dimension calculation by box-counting method.

In this approach, the log-log relationship between the number of occupied boxes $N(\varepsilon)$ and the inverse of the box size $1/\varepsilon$ is plotted. The slope of the linear fit was used to determine the fractal dimension (D_B) as $D_B = -\text{slope}$, resulting in a fractal dimension of approximately 2.0735, as indicated in **Figure 7**. This value highlights the complexity and irregularity of the failure surface, suggesting a significant roughness across multiple scales. The strong linearity observed in the log-log plot confirms the fractal nature of the surface, and the calculated dimensions provide valuable insight into its geometric characteristics.

4.2. Semi-Variogram Analysis

The semi-variogram method by Oliver and Webster (1986) offers an alternative approach to estimating fractal dimensions [47]. The semi-variogram γ_t is com-

puted as in Equation (3-12), and for fractal profiles, fractional Brownian motion (FBM) corresponds to a specific form of the semi-variogram given by Equation (3-15) following the work of Mandelbrot *et al.* [47] [48]. To minimize variability, the analysis is typically restricted to a fraction (e.g., 10% or 25%) of the data length and employs logarithmic lag spacing to improve the robustness of least-squares regression [47]. This method is particularly effective in identifying the fractal properties of surface profiles, allowing for accurate characterization of the roughness associated with failure surfaces, as shown in **Figure 8**.

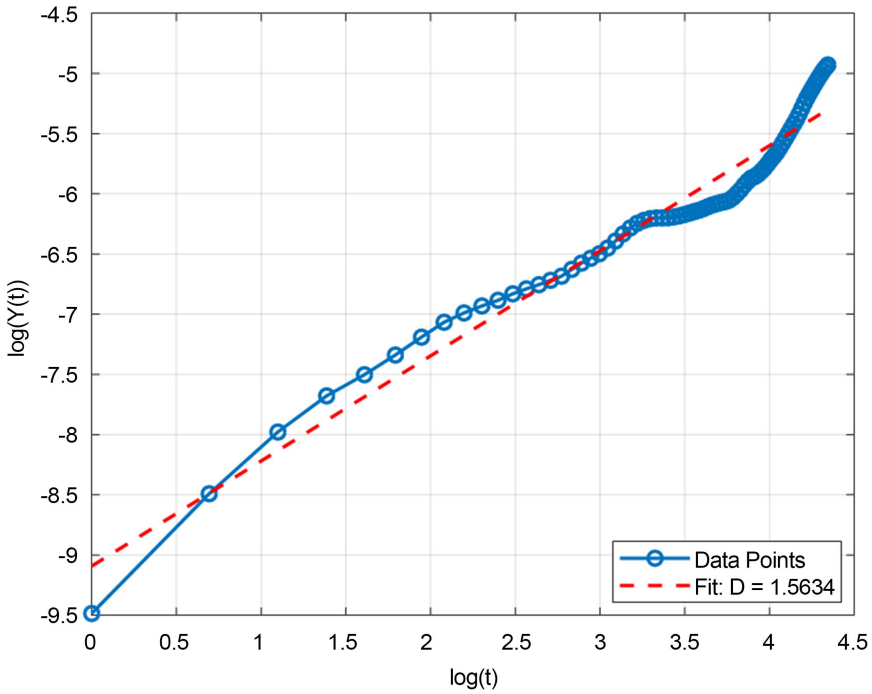

Figure 8. Fractal dimension calculation by semi-variogram method.

The slope of this linear fit was used to calculate the Hurst exponent (H), which is related to the fractal dimension (D) using the equation $D = 2 - H$, yielding a fractal dimension of approximately 1.5634, as shown in **Figure 8**. This value indicates that the failure surface was self-affine and exhibited moderate roughness and heterogeneity. The deviations from linearity observed at larger lag distances are likely to be due to boundary effects or data limitations.

5. Results and Discussions

5.1. Results

This study used high-resolution profiles to investigate the surface roughness and fractal properties of the failure surface of the Mashamba West mine. A comprehensive approach was developed to analyze the different aspects of the failure surface. Thus, it provides valuable information regarding the characteristics of the failure surface and its significance in slope stability analysis. Surface roughness

analysis (Figure 2) shows that the surface has moderate variability and localized heterogeneity at surface elevations. The mean absolute deviation (MAD) of 0.83, and the mean standard deviation (MSD) of 1.04, indicating significant micro-roughness on the failure surface. These metrics can be used to quantify the degree of surface irregularity and compare the roughness of different mining regions. Analysis of the topographical extremes (Figure 3) revealed a mean peak height (MP) of 2.4828 and mean valley depth (MV) of −4.7747, which, in general, describes the shape of the topography with respect to the contact area variability. These extreme features are where stress concentration and weakness in the slope structure are likely to occur, and therefore, may significantly affect the overall stability. Geometric irregularities were assessed based on the profile slope and curvature variability (Figure 4). A standard deviation of the profile slope (PS) of 1.04 and curvature variability (PC) of 2.963 indicated substantial surface geometry irregularities relevant to deformation behaviors and sliding mechanisms. These parameters contain information about the complexity of the failure surface topography and slope movement dynamics rate. From the power spectral density (PSD) analysis (Figure 5 and Figure 6), a dominant frequency of 0.014 was found, corresponding to periodic geological structures. This reveals recurring patterns on the failure surface, which might be related to the geological formations or structural features underlying them. The log-log PSD plot had a linear slope of 0.076, consistent with the established fractal models, indicating that the object or pattern is self-similar at different scales. Fractal dimension calculations were performed using two methods to ensure robust results. The semi-variogram method yielded a fractal dimension of 1.5634 (Figure 7).

By contrast, the box-counting method yielded a value of 2.0735 (Figure 8). Both results confirm that the failure surfaces are self-affine, implying that the surface roughness has similar patterns at different scales. This fractal behavior has important implications for the scale-dependent properties of the slope and its failure mechanisms. The quantified parameters can be used to develop improved numerical slope stability models, enhance risk assessment procedures, and help develop appropriate mitigation measures. Therefore, the research findings can be directly applied to real-world engineering problems. The fractal nature of the failure surface suggests that similar patterns may also appear at different scales, which is important for both local- and extensive-scale slope stability studies. This investigation provides a detailed characterization of the fractal properties of the failure surface of the Mashamba West mine.

5.2. Discussions

This study conducted a comprehensive analysis of the failure surface of the Mashamba West mine, unveiling the fractal characteristics of the surface and quantifying its surface roughness. The surface roughness analysis revealed high micro-roughness, as indicated by the mean absolute deviation (MAD) of 0.83 and a mean standard deviation (MSD) of 1.04. These values signify the variability of surface

elevations, a measure of the surface irregularity of geological surfaces formed by weathering, faulting, and jointing processes. From these metrics, it can be deduced that the failure surface exhibits moderate variability in surface roughness and possesses complex and heterogeneous features that are of significant importance in the study of topographical intricacies of natural failure surfaces. Understanding extreme topographical features, such as a mean peak height (MP) of 2.4828 and a mean valley depth (MV) of −4.7747, is crucial. These features not only confirm the presence of high and low points on the failure surface but also underscore the importance of considering the entire spectrum of surface characteristics in any geotechnical analysis. Surface geometry, which can vary with the contact area and mechanical interactions within the rock mass, is best understood when extreme features are identified. Fractal analysis using the semi-variogram and box-counting methods revealed the self-affine nature of the failure surface. The fractal dimensions of 1.5634 and 2.0735 prove that the surface has scale-invariant properties of surface roughness; the same roughness patterns are found at different scales. This finding is consistent with previous research on geological surfaces, which found that fractal geometry can replicate the irregularity and complexity of rock masses and failure surfaces. The fractal nature of the surface indicates that small-scale irregularities such as asperities may have a structure similar to larger-scale topographical features. Thus, fractal analysis can help characterize the entire range of surface geometries. Power spectral density (PSD) analysis also supported fractal characterization and revealed a dominant frequency of 0.014, corresponding to periodic geological structures on the surface. Identifying such periodic features implies that the failure surface is formed by underlying geological formations that impose periodic patterns on the surface. These findings are similar to those of Wu *et al*. [49] [50], who reported periodic features in other geologically complex environments. This insight is important because it shows how geological structures may affect surface roughness and its evolution. The integration of fractal analysis into surface characterization represents a significant advancement over the traditional methods. Although measures such as MAD and MSD provide limited information about the surface, fractal analysis offers a more comprehensive understanding of natural surfaces. By simulating long-range correlations and scale-dependent properties, fractal analysis revealed the complex nature of surface roughness. This is particularly important in geotechnical engineering, where many surfaces exhibit fractal-like characteristics because of the complex geological processes that produce them.

In general, high-precision quantification and characterization of surface roughness are crucial for a better understanding of natural rock masses and their behavior under different loading conditions. Although this study did not directly examine the relationship between surface roughness and slope stability, detailed surface characterization suggests the influence of roughness features on mechanical properties such as shear strength, friction, and deformation. Furthermore, based on the fractal nature of the failure surface, it may be possible to develop methods for

predicting how surface irregularities at different scales affect the behavior of rock masses during mining activities, inspiring further research and practical applications. This research highlights the potential of combining fractal analysis with other geotechnical methods to develop more realistic models of rock-mass behavior. For instance, when used in conjunction with numerical modeling techniques, fractal analysis can help identify how surface roughness affects the mechanical response of rock masses under different environmental and loading conditions. Moreover, using fractal dimensions in modeling can enhance the reliability of stability assessments and lead to improved predictions of potential failure areas in open-pit mining. Other research could also focus on how surface roughness changes over time, especially in response to weathering, changes in stress, or excavation. This research can provide valuable information on the long-term behavior of open-pit slopes and the formation of failure surfaces. Furthermore, by integrating fractal analysis with real-time monitoring technologies, such as LiDAR or photogrammetry, it is possible to develop dynamic assessments of surface changes that can improve the predictive capability of slope stability models, opening up exciting avenues for future research. This study successfully demonstrated the use of advanced surface-roughness characterization techniques, particularly fractal analysis, to understand the complexity of failure surfaces. The present study offers a suitable foundation for future research and applications in geotechnical engineering, with the possibility of improving the accuracy and reliability of models describing the behavior of failure surfaces in open-pit mining.

6. Conclusions

This study provides a comprehensive characterization of the failure surface of the Mashamba West mine, focusing on the surface roughness and fractal properties. By employing advanced techniques such as fractal dimension calculations, semivariograms, box-counting methods, and power spectral density (PSD) analysis, this research has enhanced our understanding of the complex, multiscale nature of failure surfaces in open-pit mining environments. The results highlight the intricate patterns present in failure surfaces, with significant micro-roughness and geometric irregularities identified through the analysis of the mean absolute deviation (MAD), standard deviation (SD), and topographical extremes. These findings suggest that the surface roughness exhibits notable heterogeneity, which could influence the overall stability of the slope. This study demonstrated the value of fractal analysis in capturing the self-affine and scale-invariant properties of failure surfaces. The consistency between the fractal dimensions obtained using the semivariogram and box-counting methods reinforces the reliability of fractal geometry in characterizing the surface roughness of complex geological structures. Additionally, power spectral density (PSD) analysis provided further insight into the periodic features of the failure surface, contributing to the understanding of the frequency-domain characteristics of the surface. Although the influence of surface roughness on slope stability was not directly assessed in this study, the fractal

properties and topographical features identified offer important insights into the potential behavior of the failure surface. These findings underscore the importance of considering surface roughness and its multiscale behavior in future slope stability analyses and modeling efforts.

For future research, it would be valuable to explore the direct relationship between the fractal properties of failure surfaces and mechanical properties such as shear strength and deformation behavior. Further investigation into the evolution of surface roughness due to environmental factors, such as weathering and stress changes, could provide additional insights into the long-term stability of open-pit slopes. Additionally, the integration of fractal and spectral analyses with real-time monitoring techniques can enhance the prediction and assessment of slope behavior in dynamic mining environments. This research contributes significantly to the understanding of failure surface characterization using advanced fractal analysis techniques. The insights gained from this study lay the foundation for future work aimed at improving the accuracy of slope stability models and developing more effective risk assessments and mitigation strategies for open-pit mining operations.

Acknowledgements

The authors sincerely thank Sicomines Company for its invaluable contribution to this research.

Conflicts of Interest

The authors declare that they have no conflicts of interest to disclose.

AI Disclosure Statement

The authors claim to have used AI-assisted tools to create this manuscript. The manuscript's language, structure, and clarity were refined using OpenAI's ChatGPT. These edits were reviewed and approved by the authors to ensure that they met the scientific integrity of the work and the authors' original intent. Structuring content for minor technical suggestions, generating summaries, and enhancing the presentation of complex geotechnical concepts were all performed using AI tools. The authors were responsible for and validated all scientific interpretations, analyses, and conclusions. The use of AI-assisted technologies was only for improving the readability and formatting of the manuscript. AI tools were not used for data analysis, scientific modeling, or interpretation of the results. The authors are responsible for the manuscript's content, originality, accuracy, and ethical compliance.

References

[1] Boyer, D.D. and Ferguson, K.A. (2000). Important Factors to Consider in Properly Evaluating the Stability of Rock Slopes. In: *Slope Stability* 2000, American Society of Civil Engineers, 58-71. https://doi.org/10.1061/40512(289)5

[2] Bye, A.R. and Bell, F.G. (2001) Stability Assessment and Slope Design at Sandsloot Open Pit, South Africa. *International Journal of Rock Mechanics and Mining Sciences*, **38**, 449-466. https://doi.org/10.1016/s1365-1609(01)00014-4

[3] Fu, X., Sengupta, M. and Afrouz, A. (1996) Parametric Study of Variable Slope Design for a Multiple Layered Open Pit. *International Journal of Surface Mining, Reclamation and Environment*, **10**, 41-45. https://doi.org/10.1080/09208119608964793

[4] Xu, N., Zhang, J., Tian, H., Mei, G. and Ge, Q. (2016) Discrete Element Modeling of Strata and Surface Movement Induced by Mining under Open-Pit Final Slope. *International Journal of Rock Mechanics and Mining Sciences*, **88**, 61-76. https://doi.org/10.1016/j.ijrmms.2016.07.006

[5] Pan, Q., Jiang, Y. and Dias, D. (2017) Probabilistic Stability Analysis of a Three-Dimensional Rock Slope Characterized by the Hoek-Brown Failure Criterion. *Journal of Computing in Civil Engineering*, **31**, Article ID: 04017046. https://doi.org/10.1061/(asce)cp.1943-5487.0000692

[6] Yang, J., Tao, Z., Li, B., Gui, Y. and Li, H. (2012) Stability Assessment and Feature Analysis of Slope in Nanfen Open Pit Iron Mine. *International Journal of Mining Science and Technology*, **22**, 329-333. https://doi.org/10.1016/j.ijmst.2012.04.008

[7] Abedini, M.J. and Shaghaghian, M.R. (2009) Exploring Scaling Laws in Surface Topography. *Chaos, Solitons & Fractals*, **42**, 2373-2383. https://doi.org/10.1016/j.chaos.2009.03.121

[8] Anderson, S.W. (2019) Uncertainty in Quantitative Analyses of Topographic Change: Error Propagation and the Role of Thresholding. *Earth Surface Processes and Landforms*, **44**, 1015-1033. https://doi.org/10.1002/esp.4551

[9] Lindsay, J.B., Newman, D.R. and Francioni, A. (2019) Scale-Optimized Surface Roughness for Topographic Analysis. *Geosciences*, **9**, Article No. 322. https://doi.org/10.3390/geosciences9070322

[10] Shepard, M.K., Campbell, B.A., Bulmer, M.H., Farr, T.G., Gaddis, L.R. and Plaut, J.J. (2001) The Roughness of Natural Terrain: A Planetary and Remote Sensing Perspective. *Journal of Geophysical Research: Planets*, **106**, 32777-32795. https://doi.org/10.1029/2000je001429

[11] Wang, A., Wang, K. and Tsung, F. (2014) Statistical Surface Monitoring by Spatial-Structure Modeling. *Journal of Quality Technology*, **46**, 359-376. https://doi.org/10.1080/00224065.2014.11917977

[12] Alejano, L.R., Gómez-Márquez, I. and Martínez-Alegría, R. (2010) Analysis of a Complex Toppling-Circular Slope Failure. *Engineering Geology*, **114**, 93-104. https://doi.org/10.1016/j.enggeo.2010.03.005

[13] Macciotta, R., Creighton, A. and Martin, C.D. (2020) Design Acceptance Criteria for Operating Open-Pit Slopes: An Update. *CIM Journal*, **11**, 248-265. https://doi.org/10.1080/19236026.2020.1826830

[14] Menezes, D.A.d., Carneiro, S.R.C. and Meireles, B.P. (2019) Map of the Potential Geotechnical Susceptibility for Operational Pit Slopes. *REM—International Engineering Journal*, **72**, 55-61. https://doi.org/10.1590/0370-44672018720137

[15] Micklethwaite, S., Sheldon, H.A. and Baker, T. (2010) Active Fault and Shear Processes and Their Implications for Mineral Deposit Formation and Discovery. *Journal of Structural Geology*, **32**, 151-165. https://doi.org/10.1016/j.jsg.2009.10.009

[16] Carroll, M.M. (1985) Mechanics of Geological Materials. *Applied Mechanics Reviews*, **38**, 1256-1260. https://doi.org/10.1115/1.3143685

[17] Khanna, R., Sayeed, I. and Dubey, R.K. (2018) Evaluation of Deformation Modulus

for the Jointed Rock Masses Using Equivalent Continuum Approach. *Applied Mechanics and Materials*, **877**, 200-213. https://doi.org/10.4028/www.scientific.net/amm.877.200

[18] Kulatilake, P.H.S.W. (2021) 3-D Rock Mass Strength Criteria—A Review of the Current Status. *Geotechnics*, **1**, 128-146. https://doi.org/10.3390/geotechnics1010007

[19] Moldabayev, S.K., Sdvyzhkova, O.O., Babets, D.V., Kovrov, O.S. and Adil, T.K. (2021) Numerical Simulation of the Open Pit Stability Based on Probabilistic Approach. *Naukovyi Visnyk Natsionalnoho Hirnychoho Universytetu*, No. 6, 29-34. https://doi.org/10.33271/nvngu/2021-6/029

[20] Yang, G., Leung, A.K., Xu, N., Zhang, K. and Gao, K. (2019) Three-Dimensional Physical and Numerical Modelling of Fracturing and Deformation Behaviour of Mining-Induced Rock Slopes. *Applied Sciences*, **9**, Article No. 1360. https://doi.org/10.3390/app9071360

[21] Boyd, D.L., Trainor-Guitton, W. and Walton, G. (2018) Assessment of Rock Unit Variability through Use of Spatial Variograms. *Engineering Geology*, **233**, 200-212. https://doi.org/10.1016/j.enggeo.2017.12.012

[22] Fraundorf, P. (2004) Heterogeneity, and the Secret of the Sea.

[23] Hurich, C.A. and Kocurko, A. (2000) Statistical Approaches to Interpretation of Seismic Reflection Data. *Tectonophysics*, **329**, 251-267. https://doi.org/10.1016/s0040-1951(00)00198-0

[24] Agbelele, K.J., Houehanou, E.C., Ahlinhan, M.F., Ali, A.W. and Aristide, H.C. (2023) Assessment of Slope Stability by the Fellenius Slice Method: Analytical and Numerical Approach. *World Journal of Advanced Research and Reviews*, **18**, 1205-1214. https://doi.org/10.30574/wjarr.2023.18.2.0874

[25] Kulatilake, P.H.S.W. and Ankah, M.L.Y. (2023) Rock Joint Roughness Measurement and Quantification—A Review of the Current Status. *Geotechnics*, **3**, 116-141. https://doi.org/10.3390/geotechnics3020008

[26] Lovejoy, S. and Schertzer, D. (2007) Scaling and Multifractal Fields in the Solid Earth and Topography. *Nonlinear Processes in Geophysics*, **14**, 465-502. https://doi.org/10.5194/npg-14-465-2007

[27] Andrle, R. and Abrahams, A.D. (1990) Fractal Techniques and the Surface Roughness of Talus Slopes: Reply. *Earth Surface Processes and Landforms*, **15**, 287-290. https://doi.org/10.1002/esp.3290150311

[28] Burrough, P.A. (1981) Fractal Dimensions of Landscapes and Other Environmental Data. *Nature*, **294**, 240-242. https://doi.org/10.1038/294240a0

[29] Hyslip, J.P. (2002) Fractal Analysis of Track Geometry Data. *Transportation Research Record: Journal of the Transportation Research Board*, **1785**, 50-57. https://doi.org/10.3141/1785-07

[30] Li, Y., Sun, S. and Yang, H. (2020) Scale Dependence of Waviness and Unevenness of Natural Rock Joints through Fractal Analysis. *Geofluids*, **2020**, Article ID: 8818815. https://doi.org/10.1155/2020/8818815

[31] Ling, F.F. (1989) The Possible Role of Fractal Geometry in Tribology. *Tribology Transactions*, **32**, 497-505. https://doi.org/10.1080/10402008908981918

[32] Ouadfeul, S. (2019) Introductory Chapter: Fractal in Sciences. In: Ouadfeul, S.-A., Ed., *Fractal Analysis*, IntechOpen. https://doi.org/10.5772/intechopen.84368

[33] Wang, H. and Xu, Z. (2001) A Class of Rough Surfaces and Their Fractal Dimensions. *Journal of Mathematical Analysis and Applications*, **259**, 537-553. https://doi.org/10.1006/jmaa.2000.7425

[34] Sanner, A., Nöhring, W.G., Thimons, L.A., Jacobs, T.D.B. and Pastewka, L. (2022) Scale-Dependent Roughness Parameters for Topography Analysis. *Applied Surface Science Advances*, **7**, Article ID: 100190. https://doi.org/10.1016/j.apsadv.2021.100190

[35] Marx, E., Malik, I.J., Strausser, Y.E., Bristow, T., Poduje, N. and Stover, J.C. (2002) Power Spectral Densities: A Multiple Technique Study of Different Si Wafer Surfaces. *Journal of Vacuum Science & Technology B: Microelectronics and Nanometer Structures Processing, Measurement, and Phenomena*, **20**, 31-41. https://doi.org/10.1116/1.1428267

[36] Xu, J.D., Chiente, L. and Jacobi, R.D. (2002) Characterizing Fracture Spatial Patterns by Using Semivariograms. *Acta Geologica Sinica—English Edition*, **76**, 89-99. https://doi.org/10.1111/j.1755-6724.2002.tb00074.x

[37] Maus, S. (1999) Variogram Analysis of Magnetic and Gravity Data. *Geophysics*, **64**, 776-784. https://doi.org/10.1190/1.1444587

[38] Ai, T., Zhang, R., Zhou, H.W. and Pei, J.L. (2014) Box-Counting Methods to Directly Estimate the Fractal Dimension of a Rock Surface. *Applied Surface Science*, **314**, 610-621. https://doi.org/10.1016/j.apsusc.2014.06.152

[39] Foroutan-Pour, K., Dutilleul, P. and Smith, D.L. (1999) Advances in the Implementation of the Box-Counting Method of Fractal Dimension Estimation. *Applied Mathematics and Computation*, **105**, 195-210. https://doi.org/10.1016/s0096-3003(98)10096-6

[40] Li, J., Du, Q. and Sun, C. (2009) An Improved Box-Counting Method for Image Fractal Dimension Estimation. *Pattern Recognition*, **42**, 2460-2469. https://doi.org/10.1016/j.patcog.2009.03.001

[41] Song, D., Chen, Z., Ke, Y. and Nie, W. (2020) Seismic Response Analysis of a Bedding Rock Slope Based on the Time-Frequency Joint Analysis Method: A Case Study from the Middle Reach of the Jinsha River, China. *Engineering Geology*, **274**, Article ID: 105731. https://doi.org/10.1016/j.enggeo.2020.105731

[42] Cox, B.L. and Wang, J.S.Y. (1993) Fractal Surfaces: Measurement and Applications in the Earth Sciences. *Fractals*, **1**, 87-115. https://doi.org/10.1142/s0218348x93000125

[43] Liu, X., Qu, S., Chen, R. and Chen, S. (2018) Development of a Two-Dimensional Fractal Model for Analyzing the Particle Size Distribution of Geomaterials. *Journal of Materials in Civil Engineering*, **30**, Article ID: 04018175. https://doi.org/10.1061/(asce)mt.1943-5533.0002365

[44] Hai, L., Lv, Y., Tan, S. and Feng, L. (2023) Study on the Influences of the Fractal Dimension of the Root System and Slope Degree on the Slope Stability. *Scientific Reports*, **13**, Article No. 10282. https://doi.org/10.1038/s41598-023-37561-8

[45] Zheng, L., Liu, H., Zuo, Y., Zhang, Q., Lin, W., Qiu, Q., *et al*. (2022) Fractal Study on the Failure Evolution of Concrete Material with Single Flaw Based on DIP Technique. *Advances in Materials Science and Engineering*, **2022**, Article ID: 6077187. https://doi.org/10.1155/2022/6077187

[46] Bains, R. (1992) Fractal Geometry—Mathematical Foundations and Applications. *Engineering Analysis with Boundary Elements*, **9**, 366-367. https://doi.org/10.1016/0955-7997(92)90028-6

[47] Oliver, M.A. and Webster, R. (1986) Semi-Variograms for Modelling the Spatial Pattern of Landform and Soil Properties. *Earth Surface Processes and Landforms*, **11**, 491-504. https://doi.org/10.1002/esp.3290110504

[48] Mandelbrot, B.B. and Van Ness, J.W. (1968) Fractional Brownian Motions, Frac-

tional Noises and Applications. *SIAM Review*, **10**, 422-437. https://doi.org/10.1137/1010093

[49] Wu, F.T. (1999) Fractal Geometry in Rock Mechanics: A New Approach to Analyze Rock Mass Properties. *Engineering Geology*, **54**, 23-38.

[50] Wu, D.G., Gang, T.Q., Fan, X.G. and Wu, J.L. (2014) Surface Roughness Measuring Based on the Theory of Fractal Geometry. *Applied Mechanics and Materials*, **551**, 434-438. https://doi.org/10.4028/www.scientific.net/amm.551.434